

Two-Dimensional Yukawa Liquids: Correlation and Dynamics

G. J. Kalman,¹ P. Hartmann,² Z. Donkó,² and M. Rosenberg³

¹*Department of Physics, Boston College, Chestnut Hill, Massachusetts 02467, USA*

²*Research Institute for Solid State Physics and Optics of the Hungarian Academy of Sciences, H-1525 Budapest, P.O. Box 49, Hungary*

³*Department of Electrical and Computer Engineering, University of California–San Diego, La Jolla, California 92093, USA*

(Received 20 July 2003; published 10 February 2004)

A combined theoretical and molecular dynamics (MD) simulation study of the collective modes and their dispersion in a two-dimensional Yukawa system in the strongly coupled liquid state is presented. The theoretical analysis relies upon the quasilocalized charge approximation; the MD simulation generates static pair correlation functions and dynamical current-current correlation spectra.

DOI: 10.1103/PhysRevLett.92.065001

PACS numbers: 52.27.Gr, 52.27.Lw, 52.35.Fp

Complex (dusty) plasmas have by now been recognized to constitute a system of unique value for studying the physics of strongly coupled Coulomb and Yukawa systems. The validity of the model in which the role of the electrons and ions is reduced to furnishing a polarizable background, responsible for the Yukawa behavior of the grain-grain interaction, is fairly well established [1]. The trend in current laboratory experiments has been to favor two-dimensional (2D) geometries [2] over three-dimensional ones: in a 2D system the complications that originate from the anisotropy of the grain-grain interaction, due probably to ion-wake effects [3], should be absent. One of the issues in these experiments is the understanding of the excitation and propagation of waves in the system. In the strong coupling regime the constituent grains are, in principle, either in the crystalline solid or in the liquid state. Moreover, in addition to the formation of large scale ordered lattice structures, a more common structure could be an aggregate of microcrystals whose prevailing disorder makes the behavior of the aggregate quite similar to that of the liquid state.

The first theoretical analysis of the phonon spectrum of the 2D Yukawa lattice was given by Peeters and Wu [4]. An adaptation to the complex plasma scenario was worked out more recently by Wang *et al.* [5]. A recent molecular dynamics (MD) study of the lattice dynamics is due to Liu *et al.* [6]. The 2D Yukawa systems in the *liquid* phase were considered by Löwen [7] and Murillo and Gericke [8]. Reference [7] focused on the static properties of the system, while Ref. [8] also considered some features of the collective modes. This Letter is devoted to the simultaneous theoretical and computer studies of the collective modes of 2D Yukawa liquids. In addition, the simulation results for the major equilibrium and dynamical descriptors of the system (pair distribution function and dynamical current-current correlations) are also determined. Thus, the aims of this paper are the following: (i) provide a first time combined theoretical and computer simulation analysis of a physical system of great experimental interest; (ii) show that simulation data

corroborate the results of the chosen theoretical approach; (iii) demonstrate the remarkable, previously unsuspected, scaling property of the Yukawa pair correlation function; and (iv) make it possible to assess the contrasting behaviors of Yukawa systems which are, apart from dimensionality, of identical character.

In the 2D Yukawa liquid the particles interact through the potential $\phi(r) = [(Ze)^2/r] \exp(-r/\lambda_D)$, where Z is the charge number of the particles and λ_D is the screening (electronic Debye) length. The system is characterized by the coupling parameter $\Gamma = (Ze)^2/(ak_B T)$ and the screening parameter $\kappa = a/\lambda_D$, where a is the 2D Wigner-Seitz radius, $a = (n\pi)^{-1/2}$, and n is areal density. The Fourier transform of the potential is $\phi(k) = 2\pi(Ze)^2/\sqrt{\kappa^2 + k^2}$; we use relative (barred) quantities $\bar{k} = ka$ and $\bar{r} = r/a$, and the nominal plasma frequency is $\omega_p = [2\pi(Ze)^2 n/(ma)]^{1/2} = [2(Ze)^2/(ma^3)]^{1/2}$. Collisions with the neutrals and other extraneous damping effects [2] are not included in the model.

In the weakly coupled Yukawa plasma the Vlasov–random phase approximation (RPA) collective excitation is a longitudinal acoustic mode with $\omega_0^2(\mathbf{k}) = \frac{n}{m} \phi(k)k^2 = \omega_p^2 \bar{k}^2/\sqrt{\kappa^2 + \bar{k}^2}$. In the liquid phase strong coupling is expected to soften the longitudinal dispersion and generate a transverse (shear) mode, in a qualitative resemblance to the phonon spectrum of the lattice [4]. In contrast, however, to the perfect lattice that lends itself to an exact mathematical description, the theoretical analysis of the liquid requires the adoption of a model. The approach we follow is the quasilocalized charge approximation (QLCA) that has already been successfully applied to similar problems in the 3D Yukawa liquid [9,10] and to a series of other strongly coupled plasma problems [11]. While damping is not accounted for by the model, a phenomenological description of the effect of the dominant diffusional-migrational damping is discussed below.

All the information pertaining to the mode structure is contained in the dielectric matrix that has a longitudinal and a transverse element:

$$\varepsilon_{L/T}(\mathbf{k}, \omega) = 1 - \frac{\omega_0^2(\mathbf{k})}{\omega^2 - D_{L/T}(\mathbf{k})}. \quad (1)$$

Here the $D_L(\mathbf{k})$ and $D_T(\mathbf{k})$ local field functions are the respective projections of the 2D QLCA dynamical matrix $D_{\mu\nu}(\mathbf{k})$ [12], which is a functional of the equilibrium pair correlation function (PCF) $h(r)$ or its Fourier transform $h(\mathbf{k})$:

$$D_{\mu\nu}(\mathbf{k}) = -\frac{n}{m} \int d^2r M_{\mu\nu}(r) [e^{i\mathbf{k}\cdot\mathbf{r}} - 1] h(r) \quad (2)$$

with $M_{\mu\nu}(r) = \partial_\mu \partial_\nu \phi(r)$ being the dipole-dipole interaction potential associated with $\phi(r)$.

The longitudinal and transverse modes are now determined from the dispersion relations

$$\varepsilon_L(\mathbf{k}, \omega) = 0, \quad \varepsilon_T^{-1}(\mathbf{k}, \omega) = 0. \quad (3)$$

Combination of Eqs. (1)–(4) leads to the explicit expressions

$$\begin{aligned} \omega_L^2(\mathbf{k}) &= \omega_p^2 \frac{\bar{k}^2}{2} \int d\bar{r} \Lambda(\bar{k}\bar{r}, \kappa\bar{r}) [1 + h(\bar{r})], \\ \Lambda(x, y) &= \frac{e^{-y}}{x^2} \left[(1 + y + y^2) - (4 + 4y + 2y^2) J_0(x) \right. \\ &\quad \left. + (6 + 6y + 2y^2) \frac{J_1(x)}{x} \right], \end{aligned} \quad (4)$$

and

$$\begin{aligned} \omega_T^2(\mathbf{k}) &= \omega_p^2 \frac{\bar{k}^2}{2} \int d\bar{r} \Theta(\bar{k}\bar{r}, \kappa\bar{r}) [1 + h(\bar{r})], \\ \Theta(x, y) &= 2 \frac{e^{-y}}{x^2} (1 + y + y^2) [1 - J_0(x)] - \Lambda(x, y). \end{aligned} \quad (5)$$

Evaluation of these expressions requires the input of the $h(r)$ PCF's which have been obtained through the MD simulations, as explained below. The dispersion curves generated for both modes are displayed in Fig. 1. For $\kappa = 0$ the results reproduce the known 2D Coulomb dispersion [13]. With increasing κ the mode frequencies rapidly diminish and the dispersion deviates more sub-

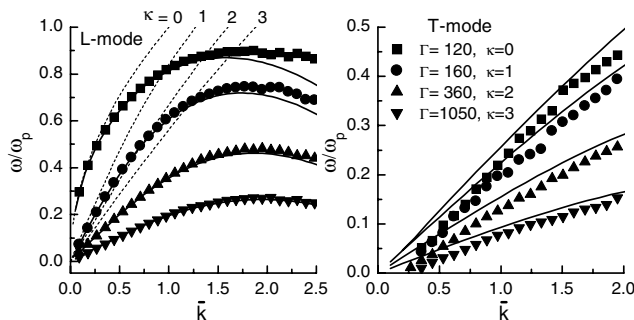


FIG. 1. Dispersion curves for the longitudinal (L) and transverse (T) modes at $\Gamma_{\text{eff}} = 120$ and $\kappa = 0, 1, 2, 3$. Continuous curves: QLCA calculations; symbols: MD simulation; dashed lines: RPA dispersions.

stantially from its RPA value. In the $k \rightarrow 0$ limit both modes exhibit an acoustic behavior, with longitudinal and transverse sound velocities s_L and s_T . For moderate κ values the sound velocities can be obtained from the semianalytic formulas [10]:

$$\begin{aligned} s_L^2 &= \frac{\omega_p^2 a^2}{\kappa} \left[1 - \frac{\kappa}{2} \left(\frac{5}{8} - \frac{\kappa^2}{2} \frac{\partial}{\partial \kappa^2} + \frac{3\kappa^4}{2} \frac{\partial^2}{\partial \kappa^4} \right) \frac{\beta |E_c|}{\Gamma} \right], \\ s_T^2 &= \frac{\omega_p^2 a^2}{2} \left(\frac{1}{8} - \frac{\kappa^2}{2} \frac{\partial}{\partial \kappa^2} - \frac{\kappa^4}{2} \frac{\partial^2}{\partial \kappa^4} \right) \frac{\beta |E_c|}{\Gamma}, \end{aligned} \quad (6)$$

where $E_c = (n/2) \int d^2r \phi(r) h(r)$ is the correlation energy per particle. The $k \rightarrow \infty$ limit of Eqs. (5) or (6) gives the average Einstein frequency (the oscillation frequency of a charge in the frozen environment of all the other particles [14]):

$$\omega_E^2 = \frac{\omega_p^2}{2} \int d\bar{r} \frac{e^{-\kappa\bar{r}}}{\bar{r}^2} [1 + \kappa\bar{r} + (\kappa\bar{r})^2] [1 + h(\bar{r})]. \quad (7)$$

The sound velocities and the Einstein frequency are shown in Fig. 2. The sound velocities obtained here are extremely close to those of the hexagonal crystal [4]. We also show the comparison with the similarly defined 3D sound velocities. The Einstein frequencies diminish rapidly with increasing κ , similarly to the 3D case [9,15].

The MD simulations are based on the particle-particle particle-mesh molecular dynamics technique, using periodic boundary conditions [16], with $N = 1600$ particles. The calculations yield the static pair correlation functions, as well as dynamical characteristics, such as spectra of the longitudinal and transverse current fluctuations, and dispersion relations for the collective excitations. Similar calculations on 3D systems have already been carried out [15,17,18].

The PCF's have been determined for a wide combination of system parameters (Γ, κ). The results for $g(r) = 1 + h(r)$ are shown in Fig. 3. We have found that within the range analyzed, for reasonably high Γ values the $g(r, \kappa, \Gamma)$ functions exhibit a universality: with an appropriately defined effective coupling $\Gamma_{\text{eff}} = \Gamma_{\text{eff}}(\Gamma, \kappa)$ (see

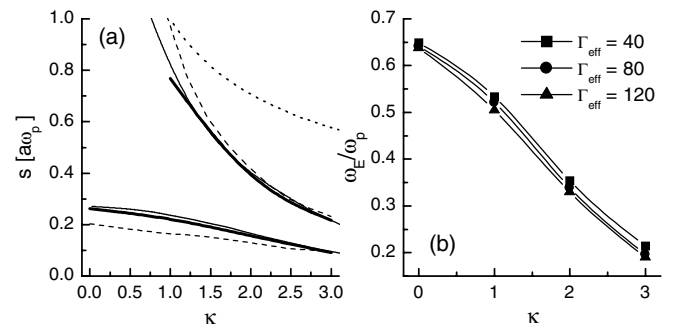


FIG. 2. (a) Sound velocities s_L (upper curves), s_T (lower curves) (heavy lines: calculated from QLCA at $\Gamma_{\text{eff}} = 120$; thin lines: for the hexagonal crystal lattice [4]; dotted line: RPA values for s_L ; and dashed lines: 3D values at $\Gamma = 160$) [9]; (b) calculated Einstein frequencies for different Γ_{eff} values.

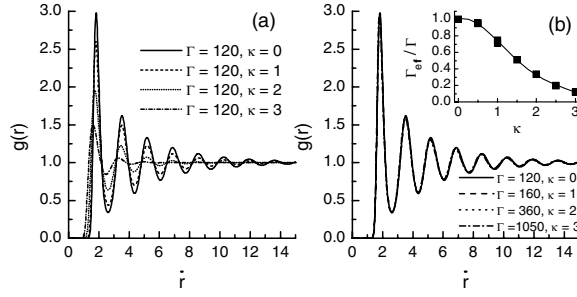


FIG. 3. Pair distribution functions; (a) variation with increasing κ at a constant $\Gamma = 120$; (b) universal pair distribution function at a constant $\Gamma_{\text{eff}} = 120$; the inset shows the dependence of $\Gamma_{\text{eff}}/\Gamma$ on κ .

inset of Fig. 3) all PCF's can be mapped, in a very good approximation, onto the Coulomb PCF. Γ_{eff} can be approximated by $\Gamma_{\text{eff}}(\Gamma, \kappa) = \Gamma f(\kappa)$ with $f(\kappa) = 1 + f_2 k^2 + f_3 k^3 + f_4 k^4$, $f_2 = -0.388$, $f_3 = 0.138$, and $f_4 = -0.0138$. (For a different definition of the effective coupling parameter in 3D systems see, e.g., [19] and references therein).

The longitudinal $L(k, \omega)$ and transverse $T(k, \omega)$ current fluctuation spectra are calculated through Fourier transform of the microscopic currents $\lambda(k, t) = k \sum_j v_{jx} \exp(ikx_j)$ and $\tau(k, t) = k \sum_j v_{jy} \exp(ikx_j)$ [assuming $\mathbf{k} = (k, 0, 0)$] [20]. The observed spectra are shown in Fig. 4 for $\Gamma_{\text{eff}} = 120$. We have verified that for this Γ_{eff} value the system is still in the liquid phase, as expected. The collective modes show up as peaks in the spectra. The peak corresponding to the longitudinal mode is much more pronounced, since this mode is maintained by the mean field, while the transverse mode is a mere correlational phenomenon.

The consistency of the MD simulation code has been checked by verifying that the dynamical structure function $S(\mathbf{k}, \omega) = (k^2/\omega^2)L(\mathbf{k}, \omega)$ satisfies the 0th and 2nd frequency moment sum rules [11,21] (as shown in Fig. 4). Note that the static structure function $S(k=0) > 0$ for $\kappa > 0$, as dictated by the compressibility sum rule. The dispersion relations for the longitudinal and for the transverse modes derived from these fluctuation spectra are displayed in Fig. 1, in combination with the theoretically predicted dispersion. At $\kappa = 0$ the known simulation results for the Coulomb system [22] are recovered. For the longitudinal mode the simulation data corroborate well the theoretical predictions, except at the highest k values where the oscillatory trend of the QLC dispersion is washed out by short range disorder. In the case of the transverse mode, the agreement between theory and MD data for moderately high k values is fairly good; for $k \rightarrow 0$ the agreement is marred by the QLCA's inability to account for diffusional and other damping effects [13] that preclude the existence of long wavelength shear waves in the liquid state. As a result of this damping, a cutoff at a finite k_* and zero frequency develops (a similar phenom-

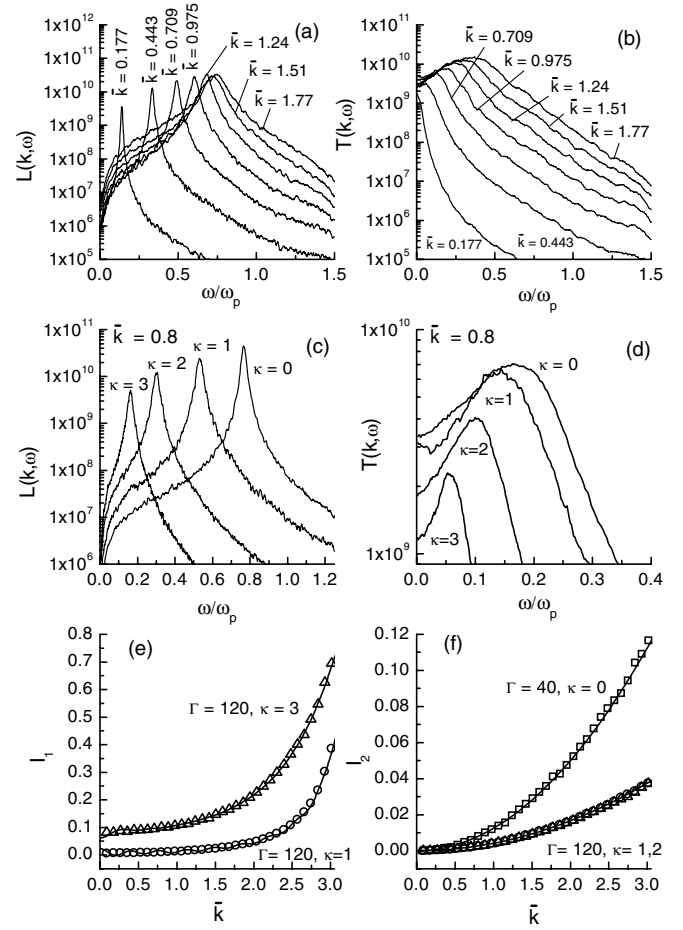


FIG. 4. (a),(c) Longitudinal and (b),(d) transverse current-current correlation functions at $\Gamma_{\text{eff}} = 120$; (a),(c) Variation with \bar{k} at $\kappa = 1$. (b),(d) Variation with κ at $\bar{k} = 0.8$. (e),(f) The satisfaction of the 0th and 2nd frequency moment sum rules: the continuous lines represent the theoretical expectations; the symbols are the calculated moments.

non was observed in the 3D case [15,17]). The k_* value is related to the diffusional-migrational time [13] through $\tau_{\text{DM}} = 1/k_* s_T$, where s_T is the transverse sound velocity. The value τ_{DM} , calculated with the aid of the theoretically predicted s_T values, is shown in the inset of Fig. 5. If this τ_{DM} value is incorporated in the QLCA equations as a phenomenological damping $\nu = 1/\tau_{\text{DM}}$ [by the $\omega \rightarrow \omega + i\nu$ replacement in the denominator of Eq. (1)], the good agreement between the theory and the MD data is restored (Fig. 5). The simulations show that the longitudinal mode is not affected by this damping mechanism: this may indicate that its characteristic damping time is substantially longer.

At the present time, there exist quite a few experimental results on collective modes in small 2D crystals [2] but observations on liquids or larger scale aggregates of microcrystals are lacking (observations of waves in strongly coupled 3D liquid were reported in [23]). In order to pursue experiments on a liquid at a constant Γ_{eff} , say, at

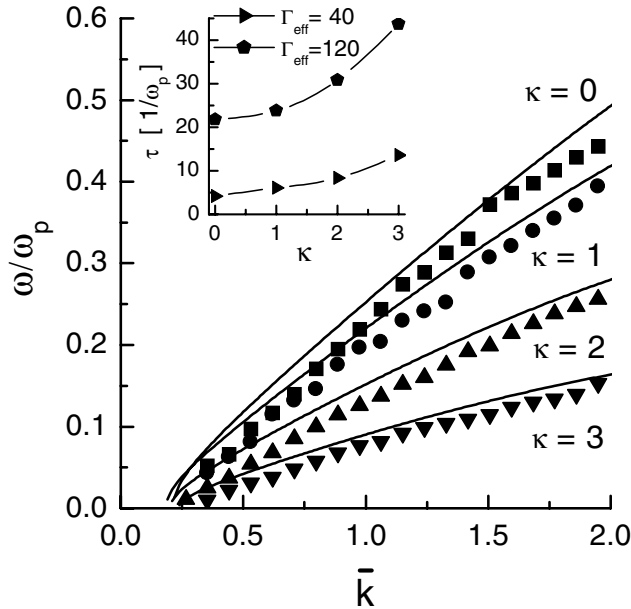


FIG. 5. Shear mode dispersion calculated from the modified QLCA with a phenomenological damping (continuous lines), the symbols show the results of the MD simulation; the inset portrays the variation of the migrational-diffusional time constant, estimated from the cutoff wave number of the shear mode.

$\Gamma_{\text{eff}} = 120$ value, and explore the effect of the changing screening parameter κ , one might consider varying grain size and grain density simultaneously (without changing the parameters of the background plasma). For example, consider a dusty argon plasma, with neutral density $n_n \sim 10^{14} \text{ cm}^{-3}$ ($P \sim 3 \text{ mTorr}$), plasma density $n_e \sim 10^8 \text{ cm}^{-3}$, and $T_e \sim 2 \text{ eV}$: here, the electron Debye length $\lambda_D \sim 0.1 \text{ cm}$. Dust grains with $R \sim 0.6 \mu\text{m}$, $Z \sim 2000$, and $n \sim 32 \text{ cm}^{-2}$ could yield a liquid state with $\kappa \sim 1$ and $\Gamma \sim 180$; a smaller density of larger dust grains ($R \sim 1 \mu\text{m}$, $Z \sim 4000$, $n \sim 8 \text{ cm}^{-2}$) could yield $\kappa \sim 2$ and $\Gamma \sim 380$. With the above values, and with dust mass density $\sim 1.5 \text{ g/cm}^3$, the ratio of the dust-neutral hard-sphere collision frequency, $[\nu_{dn} \sim (4\pi/3)R^2 n_n v_n m_n/m]$ to the dust plasma frequency is roughly ≤ 0.1 , consistent with the collisionless theoretical picture.

In summary, we have given a detailed analysis of the collective mode structure of a strongly coupled 2D Yukawa liquid, based on combined theoretical analysis and computer simulation. Results derived from the two approaches are in good agreement with each other. We suggest that experimental verification of these results should be possible.

This work has been partially supported by NSF Grant No. PHYS-0206695, NSF Grant No. INT-0002200, DOE

Grant No. DE-FG02-03ER54716, Grant No. OTKA-T-34156, Grant No. MTA-NSF-OTKA-028, DOE Grant No. DE-FG03-97-ER54444, and DOE Grant No. DE-FG02-03ER54730. G.J.K. thanks Kenneth Golden for useful discussions.

- [1] U. Konopka, G. E. Morfill, and L. Ratke, Phys. Rev. Lett. **84**, 891 (2000).
- [2] S. Nunomura, D. Samsonov, and J. Goree, Phys. Rev. Lett. **84**, 5141 (2000); S. Nunomura *et al.*, Phys. Rev. Lett. **89**, 035001 (2002); A. Homann *et al.*, Phys. Lett. A **242**, 173 (1998); S. Nunomura *et al.*, Phys. Rev. E **65**, 066402 (2002).
- [3] M. Lampe *et al.*, Phys. Plasmas **7**, 3851 (2000).
- [4] F. M. Peeters and X. Wu, Phys. Rev. A **35**, 3109 (1987).
- [5] X. Wang, A. Bhattacharjee, and S. Hu, Phys. Rev. Lett. **86**, 2569 (2001).
- [6] Y. Liu *et al.*, Phys. Rev. E **67**, 066408 (2003).
- [7] H. Löwen, J. Phys. Condens. Matter **4**, 10105 (1992).
- [8] M. S. Murillo and D. O. Gericke, J. Phys. A **36**, 6273 (2003).
- [9] G. Kalman, M. Rosenberg, and H. E. DeWitt, Phys. Rev. Lett. **84**, 6030 (2000).
- [10] M. Rosenberg and G. Kalman, Phys. Rev. E **56**, 7166 (1997).
- [11] K. I. Golden and G. J. Kalman, Phys. Plasmas **7**, 14 (2000).
- [12] G. J. Kalman and K. I. Golden, Phys. Rev. A **41**, 5516 (1990).
- [13] K. I. Golden, G. J. Kalman, and P. Wyns, Phys. Rev. A **41**, 6940 (1990); **46**, 3463 (1992).
- [14] Z. Donkó, P. Hartmann, and G. J. Kalman, Phys. Plasmas **10**, 1563 (2003); B. Bakshi, Z. Donkó, and G. J. Kalman, Contrib. Plasma Phys. **43**, 261 (2003).
- [15] H. Ohta and S. Hamaguchi, Phys. Rev. Lett. **84**, 6026 (2000); T. Saigo and S. Hamaguchi, Phys. Plasmas **9**, 1210 (2002).
- [16] R. W. Hockney and J. W. Eastwood, *Computer Simulation Using Particles* (McGraw-Hill, New York, 1981).
- [17] M. S. Murillo, Phys. Rev. Lett. **85**, 2514 (2000); K. Y. Sanbonmatsu and M. S. Murillo, Phys. Rev. Lett. **86**, 1215 (2001).
- [18] A. Wierling, T. Pschiwul, and G. Zwicknagel, Phys. Plasmas **9**, 4871 (2002); A. Wierling, T. Saigo, and S. Hamaguchi (to be published).
- [19] V. E. Fortov *et al.*, Phys. Rev. Lett. **90**, 245005 (2003).
- [20] See, e.g., J.-P. Hansen, I. R. McDonald, and E. L. Pollock, Phys. Rev. A **11**, 1025 (1975); S. Hamaguchi, Plasmas Ions **2**, 57 (1999).
- [21] Z. Donkó *et al.*, Phys. Rev. Lett. **90**, 226804 (2003).
- [22] H. Totsuji and N. Takeya, Phys. Rev. A **22**, 1220 (1980).
- [23] J. Pramaniket *et al.*, Phys. Rev. Lett. **88**, 175001 (2002).